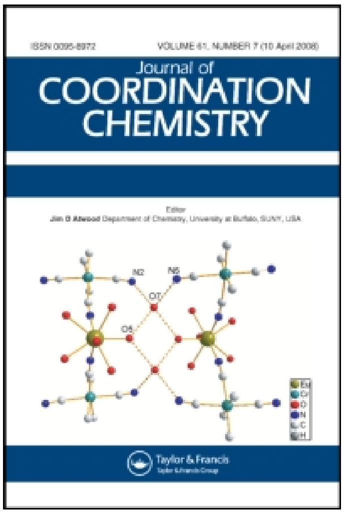

Journal of Coordination Chemistry
Publication details, including instructions for authors and subscription information:
http://www.informaworld.com/smpp/title~content=t713455674

A novel carboxylic coordination polymer of samarium(III): [Sm(H$_{\text{2}}$O)(4,4'-bipyridine)(CCl$_{\text{2}}$HCOO)$_{\text{3}}$]$_{\text{n}}$

Rafal Kruszynski[a]; Agnieszka Czylkowska[a]; Danuta Czakis-Sulikowska[a]
[a] Institute of General and Ecological Chemistry, Lodz University of Technology, 90-924, Łódź, Poland

To cite this Article Kruszynski, Rafal , Czylkowska, Agnieszka and Czakis-Sulikowska, Danuta(2006) 'A novel carboxylic coordination polymer of samarium(III): **[Sm(H$_{\text{2}}$O)(4,4'-bipyridine)(CCl$_{\text{2}}$HCOO)$_{\text{3}}$]$_{\text{n}}$**', Journal of Coordination Chemistry, 59: 6, 681 — 690

To link to this Article: DOI: 10.1080/00958970500345356

URL: http://dx.doi.org/10.1080/00958970500345356

Journal of Coordination Chemistry
Vol. 59, No. 6, 15 April 2006, 681–690

A novel carboxylic coordination polymer of samarium(III): $[Sm(H_2O)(4,4'\text{-bipyridine})(CCl_2HCOO)_3]_n$

RAFAL KRUSZYNSKI*, AGNIESZKA CZYLKOWSKA
and DANUTA CZAKIS-SULIKOWSKA

Institute of General and Ecological Chemistry, Lodz University of Technology,
90-924, Łódź, Poland

(*Received in final form 7 July 2005*)

A novel mixed ligand complex $[Sm(H_2O)(4,4'\text{-bpy})(CCl_2HCOO)_3]_n$ has been synthesized and characterized by elemental and thermal analysis, IR and conductivity studies. A coupled TG–MS system was used to monitor principal volatile fragments evolved during pyrolysis. The crystal and molecular structure of the complex was determined. The samarium atom is nine coordinated by two oxygen atoms from one chelating tridentate dichloroacetate ligand, four oxygen atoms from four bidentate bridging dichloroacetate groups, one oxygen atom from a bridging tridentate dichloroacetate ligand, one water molecule and one nitrogen atom from 4,4′-bipyridyl. The coordination polyhedron can be described as tricapped trigonal prism, distorted towards a capped tetragonal antiprism. Molecules are linked up by O–H···N hydrogen bonds and stacking interactions to give a two-dimensional net.

Keywords: Samarium(III); 4,4′-Bipyridine; Dichloroacetate; Thermal decomposition; Crystal structure; Valence

1. Introduction

For many years attention has been focused on lanthanide complexes, because of their applications in diagnostic medicine (e.g., contrast agents for magnetic resonance imaging [1, 2], radiotherapeutic drugs [3], fluoroimmunoassay [4]), in hetero- and homogeneous catalysis [5, 6], as components of permanent magnetic materials [7], and so on. Generally, lanthanide ions interact with ligands in a largely electrostatic way. This results in a high degree of liability in most lanthanide complexes and lanthanide ions are kinetically stable only in compounds containing chelating ligands. Metal-to-ligand bonding mostly involves d-orbitals (f-orbitals practically do not participate into bond creation) and the coordination geometry of lanthanide complexes is dominated by steric effects. Ligand assembly around lanthanide ions is determined

---

*Corresponding author. Email: kruszyna@p.lodz.pl

ISSN 0095-8972 print: ISSN 1029-0389 online © 2006 Taylor & Francis
DOI: 10.1080/00958970500345356

by the tendency to minimise interligand repulsions, and the coordination number (CN) is strongly limited by the steric bulk of the ligands. CNs usually vary from 8 to 13 and coordination geometries are often irregular. Lower CNs can be achieved only with very bulky ligands and the highest CNs are usually associated with chelating ligands that have small bite-angles, such as nitrate ion [8]. Lanthanide ions, as typical hard Lewis acids, display strong affinity for O-donor ligands. With larger CNs, water molecules are often coordinated beside the organic and inorganic ligands. In lanthanide chemistry, the geometry and arrangement of ligands in the inner coordination sphere is of special importance in relation to applications in ion extraction and separation processes and in magnetic resonance imaging [9–14]. Introduction of uncharged ligands possessing donor electron properties to the inner coordination sphere can affect not only the coordination sphere itself, but also assembly of polymeric species in various supramolecular motifs. As a model ligand in our investigation of such species, reported below, we chose 4,4′-bipyridyl (4-bpy) because of its tendency to create polymeric species [15–18]. Coordination polymers possessing rigid or flexible chains/nets [19–22] and capable of creating nanoporous channels are of great interest due to their unique properties such as gas adsorption [22–37], chemical adsorption [22, 23, 38–42], ion-exchange [43–46] and heterogeneous catalysis [20, 47–48].

2. Experimental

2.1. *Chemicals*

4,4′-Bipyridine, dichloroacetic acid and $SmCl_3 \cdot 6H_2O$ were obtained from Aldrich; methanol, dimethyloformamide and dimethylosulfoxide from Lab. Scan, Reachim and VEB Jano-pharm Labochem Apolda. $Sm(OH)_3$ was obtained by reacting samarium chloride with solution of NaOH. A solution of samarium(III) dichloroacetate was prepared by dissolving freshly precipitated $Sm(OH)_3$ in 2 M dichloroacetic acid in stoichiometric quantities (pH $\sim$4.0). The samarium content was determined complexometrically with standard EDTA solution, using xylenol orange as an indicator. Other chemicals were of analytical reagent grade from POCh-Gliwice.

2.2. *Synthesis*

A solution of 4-bpy (6.2 mmol) in 96% v/v ethanol (11 cm^3) was added to a freshly prepared solution of samarium(III) dichloroacetate (3.1 mmol) in water (29 cm^3) at room temperature. Over a period of several days a crystalline complex was obtained. The colourless product was filtered off, washed with cold EtOH, ethanol–diethylether (1/1; v/v) and dried in air. C, H and N were determined by elemental analysis with V_2O_5 as oxidizing agent; Sm(III) was determined complexometrically. Anal. Calcd for $[Sm(H_2O)(C_{10}H_8N_2)(C_6H_3O_6Cl_6)_3]$ (%): Sm, 21.23; C, 27.13; H, 1.85; N, 3.95. Found: Sm, 21.26; C, 27.00; H, 1.91; N, 4.11.

2.3. *Crystal structure determination*

A colourless rectangular prism was mounted on a KM-4-CCD automatic diffractometer equipped with a CCD detector. X-ray intensity data were collected with

Table 1. Crystal data and structure refinement details for the complex.

Empirical formula	$(C_{16}H_{13}Cl_6N_2O_7Sm)_n$
Formula weight	708.33
Temperature (K)	293.0(2)
Wavelength (Å)	λ(Mo Kα) = 0.71073
Crystal system, space group	Triclinic, $P\bar{1}$
Unit cell dimensions (Å, °)	$a = 9.4478(6)$ $b = 10.6972(6)$ $c = 12.3844(7)$ $\alpha = 103.674(5)$ $\beta = 99.851(5)$ $\gamma = 93.533(5)$
Volume (Å^3)	1191.39(12)
Z, Calculated density (Mg m^{-3})	2, 1.975
Absorption coefficient (mm^{-1})	3.177
F(000)	686
Crystal size (mm)	0.201 × 0.425 × 0.639
θ range for data collection	3.24 to 25.10
Index ranges	$-8 \le h \le 11$, $-12 \le k \le 12$, $-14 \le l \le 14$
Reflections collected/unique	10987/4225 [$R_{(int)} = 0.0288$]
Completeness to $2\theta = 25.11°$	99.4%
Refinement method	Full-matrix least-squares on F^2
Max. and min. transmission	0.584 and 0.213
Data/restraints/parameters	4225/0/208
Goodness-of-fit on F^2	1.048
Final R indices [$I > 2\sigma(I)$]	$R_1 = 0.0263$, $wR_2 = 0.0620$
R indices (all data)	$R_1 = 0.0270$, $wR_2 = 0.0626$
Largest diff. peak and hole (e Å^{-3})	1.249 and −0.747

graphite-monochromated Mo Kα radiation ($\lambda = 0.71073$ Å) at 293.0(2) K, with the ω scan mode. An 11 seconds exposure time was used and the whole Ewald sphere was collected up to $2\theta = 50.2°$. Unit cell parameters were determined from least-squares refinement of the setting angles of 10213 strongest reflections. Details concerning crystal data and refinement are given in table 1. Examination of two reference frames monitored after each 20 frames measured showed 17.2% loss of intensity. During data reduction this decay was taken into account. Lorentz, polarization, and numerical absorption [49] corrections were applied. The structure was solved by direct methods. All non-hydrogen atoms were refined anisotropically using full-matrix, least-squares techniques on F^2. All hydrogen atoms were found from difference Fourier syntheses after four cycles of anisotropic refinement, and refined as riding on the adjacent atom with individual isotropic displacement factors equal to 1.2 times the value of equivalent displacement factor of the carbon atom (1.5 times for oxygen). SHELXS97 [50], SHELXL97 [51] and SHELXTL [52] programs were used for all calculations. Atomic scattering factors were those incorporated in the computer programs. Selected interatomic bond distances and angles are listed in table 2.

2.4. *Other measurements*

Elemental analyses were carried out using a Carbo-Erba instrument. IR spectra (KBr pellets) were obtained using a Shimadzu spectrophotometer (4000–400 cm^{-1}). Conductivity measurements were performed on an OK-102/1 conductivity meter equipped with an OK 902 electrode at 298.14 ± 0.05 K. Molar conductivity (Λ_M) was

Table 2. Selected bond lengths and angles (Å, °) for the complex.

Sm(1)–O(1)	2.474(2)	C(1)–C(2)	1.380(5)
Sm(1)–O(2)#1	2.397(2)	C(2)–C(3)	1.400(5)
Sm(1)–O(3)#1	2.409(3)	C(3)–C(4)	1.385(5)
Sm(1)–O(3)	2.868(3)	C(4)–C(5)	1.378(5)
Sm(1)–O(4)	2.503(3)	O(1)–C(11)	1.250(4)
Sm(1)–O(5)	2.407(2)	O(2)–C(11)	1.243(4)
Sm(1)–O(6)#2	2.423(2)	O(4)–C(13)	1.232(5)
Sm(1)–O(7)	2.471(3)	O(3)–C(13)	1.247(5)
Sm(1)–N(1)	2.688(3)	O(6)–C(15)	1.240(4)
N(1)–C(5)	1.343(5)	O(5)–C(15)	1.259(4)
N(1)–C(1)	1.344(5)		
O(2)#1–Sm(1)–O(5)	137.76(8)	O(6)#2–Sm(1)–O(4)	145.43(9)
O(2)#1–Sm(1)–O(3)#1	70.76(9)	O(7)–Sm(1)–O(4)	130.58(10)
O(5)–Sm(1)–O(3)#1	145.46(9)	O(1)–Sm(1)–O(4)	71.28(9)
O(2)#1–Sm(1)–O(6)#2	76.70(9)	O(2)#1–Sm(1)–N(1)	70.01(9)
O(5)–Sm(1)–O(6)#2	83.81(8)	O(5)–Sm(1)–N(1)	68.83(9)
O(3)#1–Sm(1)–O(6)#2	86.72(10)	O(3)#1–Sm(1)–N(1)	139.44(9)
O(2)#1–Sm(1)–O(7)	135.54(10)	O(6)#2–Sm(1)–N(1)	74.71(9)
O(5)–Sm(1)–O(7)	70.61(9)	O(7)–Sm(1)–N(1)	130.57(9)
O(3)#1–Sm(1)–O(7)	74.85(10)	O(1)–Sm(1)–N(1)	137.22(9)
O(6)#2–Sm(1)–O(7)	73.99(9)	O(4)–Sm(1)–N(1)	70.73(9)
O(2)#1–Sm(1)–O(1)	129.84(8)	O(2)#1–Sm(1)–O(3)	68.56(9)
O(5)–Sm(1)–O(1)	88.18(8)	O(5)–Sm(1)–O(3)	128.88(8)
O(3)#1–Sm(1)–O(1)	78.17(9)	O(3)#1–Sm(1)–O(3)	73.45(11)
O(6)#2–Sm(1)–O(1)	140.17(8)	O(6)#2–Sm(1)–O(3)	144.00(8)
O(7)–Sm(1)–O(1)	66.57(9)	O(7)–Sm(1)–O(3)	126.33(8)
O(2)#1–Sm(1)–O(4)	91.55(11)	O(1)–Sm(1)–O(3)	65.31(8)
O(5)–Sm(1)–O(4)	83.69(9)	O(4)–Sm(1)–O(3)	47.44(9)
O(3)#1–Sm(1)–O(4)	120.32(10)	N(1)–Sm(1)–O(3)	101.12(9)

Symmetry transformations used to generate equivalent atoms are #1: $-x, -y+1, -z+1$; #2: $-x+1, -y+1, -z+1$.

measured using 10^{-3} M solutions in MeOH, DMF and DMSO. Thermal decomposition studies were carried out on a Q-1500 derivatograph over the temperature range 293–1273 K at a heating rate of 10 K min^{-1} in static air. The sample mass was 100 mg; α-Al_2O_3 served as reference. Thermal decomposition products were confirmed by recording IR spectra of sinters prepared by heating samples to fixed temperatures. In the sinter the presence of Cl^- was also investigated. The TG-MS system used to monitor volatile products produced during pyrolysis consisted of a TG/DTA (SETSYS-16/18) coupled to a mass spectrometer (QMS-422; ThermoStar Balzers Instruments). Dynamic measurements were carried out in air at a flow rate of 1 dm^3 h^{-1}.

3. Results and discussion

The colourless complex is air stable at room temperature. Its molar conductance (Ω^{-1} cm^2 mol^{-1}) in MeOH (51.3) and DMF (54.5) indicates behaviour intermediate between non- and 1 : 1 electrolytes [53]. The molar conductivity in DMSO (52.5) corresponds to a 1 : 1 electrolyte. Higher than anticipated Λ_M values are probably due to displacement of dichloroacetate ligands solvent.

A perspective view of the asymmetric unit of the unit cell together with the atom numbering scheme is shown in figure 1, with displacement ellipsoids plotted

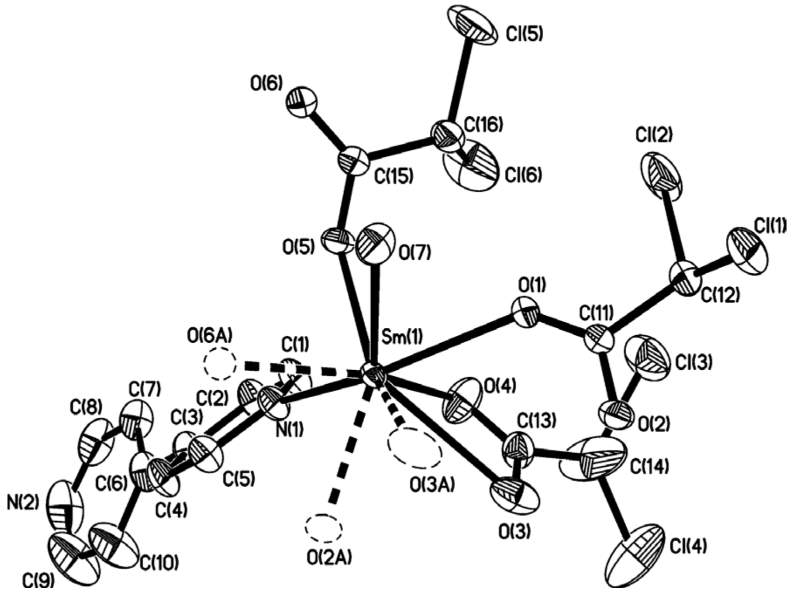

Figure 1. A perspective view of the complex with atom numbering, plotted with 50% probability displacement ellipsoids. Hydrogen and disordered chlorine atoms are omitted for clarity. Symmetry-generated atoms are indicated by dashed lines.

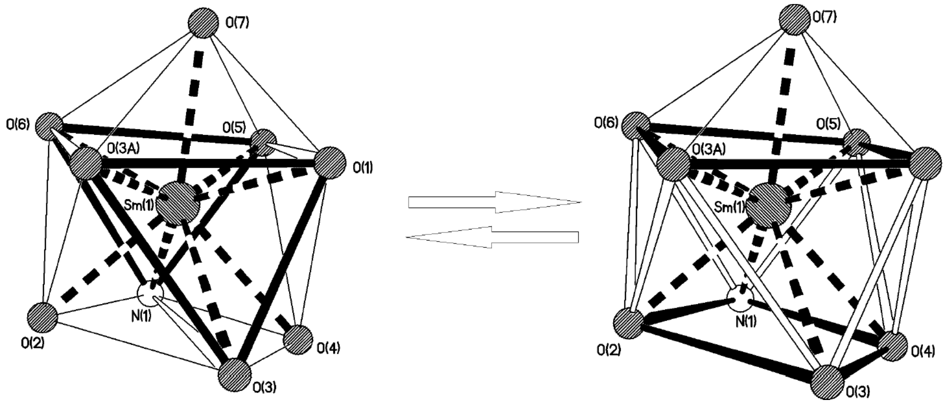

Figure 2. The samarium coordination polyhedron as a tricapped trigonal prism (left) distorted toward a capped tetragonal antiprism (right).

at 50% probability. In one of the dichloroacetate substituents (indicated by the C(13) atom) chlorine atoms are disordered over two positions. The samarium atom is nine coordinated by two oxygen atoms from one chelating tridentate dichloroacetate ligand, four oxygen atoms from four bidentate bridging dichloroacetate groups, one oxygen atoms from one bridging tridentate dichloroacetate ligand, one water molecule and one nitrogen atom from 4,4′-bipyridyl. The coordination polyhedron can be described as tricapped trigonal prism distorted toward a capped tetragonal antiprism (figure 2) [54]. Inversion centres (special positions *g* and *h* of space group $P\overline{1}$ at 0, 1/2, 1/2 and 1/2, 1/2, 1/2 [55]) connect molecules to form a one-dimensional

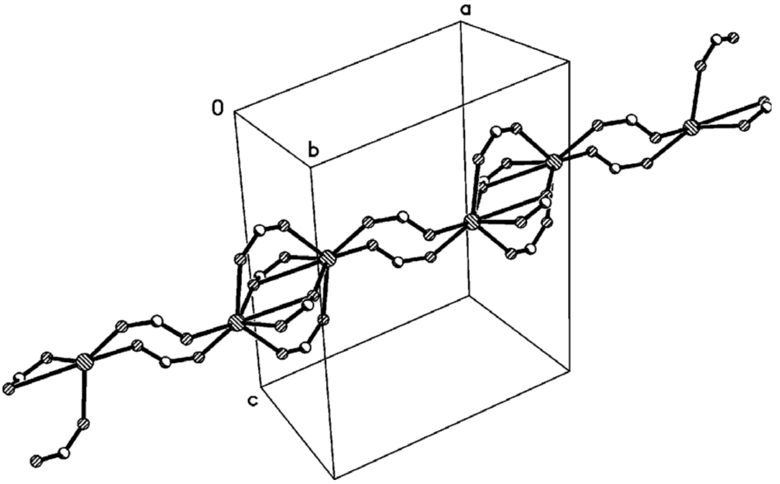

Figure 3. The coordination polymer chain created along the *a* direction.

coordination polymer along the *a* direction (figure 3). This is first known lanthanide coordination polymer containing one additional chelating and bridging carboxylic groups per central atom, apart from the main chain created by bridging carboxylic groups. These additional groups create supplementary stabilization to every second polymer chain mesh. All chain carboxylate polymers of lanthanides reported in the literature have two [56–63] or three [64] chelating carboxylic groups, or different numbers of chelating groups for different coordination centres within one molecule [65, 66]. In the present complex, each main chain mesh is created from eight atoms (two samarium, two carbon and four oxygen). All except chelating, carboxylic groups are bonded symmetrically to the central atoms. The planar (within experimental error) piridyl rings are inclined at 36.85(18)°.

Bond valences were computed as $\nu_{ij} = \exp[(R_{ij} - d_{ij})/0.37]$ [67–69], where R_{ij} is the bond-valence parameter (in the formal sense R_{ij} can be considered as a parameter equal to the idealised single-bond length between *i* and *j* atoms). $R_{\mathrm{Sm-O}}$ and $R_{\mathrm{Sm-N}}$ were taken as 2.063 [70] and 2.171 [71], respectively. Computed bond valences for samarium are $\nu_{\mathrm{Sm(1)-O(1)}} = 0.329$, $\nu_{\mathrm{Sm(1)-O(2;}-x,-y+1,-z+1)} = 0.405$, $\nu_{\mathrm{Sm(1)-O(3)}} = 0.393$, $\nu_{\mathrm{Sm(1)-O(3;}-x,-y+1,-z+1)} = 0.114$, $\nu_{\mathrm{Sm(1)-O(4)}} = 0.304$, $\nu_{\mathrm{Sm(1)-O(5)}} = 0.395$, $\nu_{\mathrm{Sm(1)-O(6;}-x+1,-y+1,-z+1)} = 0.378$, $\nu_{\mathrm{Sm(1)-O(7)}} = 0.332$, $\nu_{\mathrm{Sm(1)-N(1)}} = 0.247$ valence units, and thus the computed valence of the Sm(1) atom is 2.90. The deviation of valence sum rule can be explained by constraints imposed by tridentate carboxylic groups. The weakest is the bridge bond between samarium and $\mathrm{O}(3; -x, -y+1, -z+1)$; the Sm-bipyridyl bond is almost twice as strong and the rest about three times stronger.

In the structure there exist intramolecular O(water)–H···O(carboxyl) hydrogen bonds and weak intramolecular C–H···O, C–H···Cl hydrogen bonds [72–74] (table 3), which provide additional stabilization of the polymeric chains. The molecules of title compound are further connected by strong O(water)–H···N(bipyridyl) hydrogen bonds (for details see table 3) and stacking interactions [75] between pyridine rings (the Cg···Cg# distance is equal to 4.560(5) Å and the angle between the Cg···Cg# vector and the normal to the plane is 40.54(8)°; the perpendicular distance from Cg to the infinite two-dimensional net along the crystallographic $[0\ 1\ \bar{1}]$ plane (figure 4)

Table 3. Hydrogen bonding details for the complex (Å, °).

D–H···A	d(D–H)	d(H···A)	d(D···A)	∠(DHA)
O(7)–H(7O)···O(5)#2	0.95	2.21	2.859(4)	125.0
O(7)–H(7P)···N(2)#3	0.78	2.05	2.774(5)	153.4
C(16)–H(16)···Cl(2)	0.98	2.7	3.477(4)	136.8
C(16)–H(16)···O(1)	0.98	2.45	3.343(5)	151.9

Symmetry transformations used to generate equivalent atoms are #2: $-x+1, -y+1, -z+1$; #3: $x, y+1, z+1$.

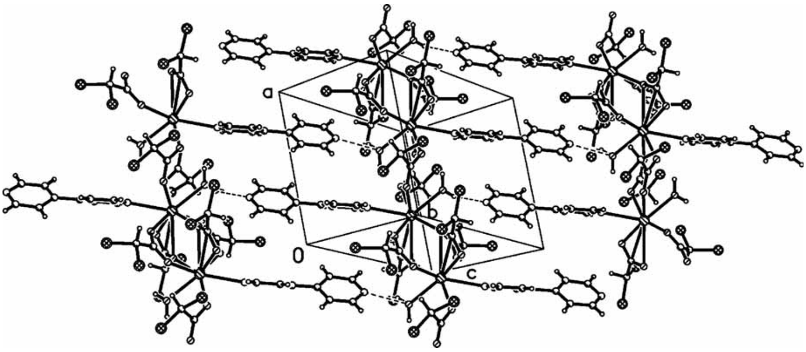

Figure 4. Crystal packing of the complex showing the channel mesh created along the $[0\ 1\ \bar{1}]$ direction. Hydrogen bonds are indicated by dashed lines.

is 3.466(5) Å). In this way, approximately rectangular channels are created along the $[0\ 1\ \bar{1}]$ direction. These channels have two different sizes, $13.198(5) \times 3.528(6)$ and $7.904(5) \times 4.397(5)$ Å, and are bordered by pyridyl residues, thus suggesting the possibility of using the complex for selective absorption and heterogeneous catalysis.

IR spectra of the complex exhibit several bands characteristic of 4-bpy and dichloroacetate groups. The infrared spectrum of free 4-bpy undergoes a change upon coordination. The characteristic ring stretching vibration modes ν(CC), ν(CN), $\nu(\mathrm{CC})_{\mathrm{inter\ ring}}$ (A_1 symmetry) and ν(CC), ν(CN) (B_1 symmetry) appear at 1588 and 1530 cm^{-1} in the free ligand [76]. In IR spectra of the compound, they are observed at 1605 (A_1 symmetry) and 1533 cm^{-1} (B_1 symmetry), respectively. The ring "breathing" mode is shifted by 15 cm^{-1} towards higher frequencies in comparison to free 4-bpy. This bathochromic shift is consistent with coordination of 4-bpy [77].

Asymmetric stretching modes (ν_{as}OCO) are split and appear at 1688 and 1620 cm^{-1}. The latter is strongly linked to 4-bpy ring stretching modes ν(CC), ν(CN), $\nu(\mathrm{CC})_{\mathrm{inter\ ring}}$ at 1605 cm^{-1}. Symmetric stretching modes (ν_{s}OCO) are superimposed on 4-bpy absorptions. Thus from IR data it is difficult to discuss the nature of Sm(III)–dichloroacetate bonds. The compound exhibits a band in the water stretching region at ca 3460 cm^{-1}. H_2O wagging vibrations for coordinated water were not observed.

Thermal decomposition of the complex in air is a multi-stage process (general scheme below). The compound is stable to 373 K. The first mass loss is assigned to water evolution (Calcd 2.54%, found 2.5% in the temperature range 373–423 K). With increasing temperature (453–548 K) partial decomposition of the dichloroacetate ligands take place. During this process, the intermediate species $\mathrm{Sm(4\text{-}bpy)(Cl_2CHCOO)Cl_2}$ is probably formed (Calcd 26.11%, found 26.0%). In the sinter heated to 513 K, absorption bands for 4-bpy and dichloroacetate groups were found and chlorine ions were present. In the range 548–1093 K, SmOCl begins to form and above 1093 K Sm_2O_3 was identified as the final product of decomposition (Calcd 3.88%, found. 3.5%). Pyrolysis is accompanied by several exo- and endothermic effects in the DTA curve (given in the scheme below).

$$\mathrm{Sm(H_2O)(4\text{-}bpy)(CCl_2HCOO)_3} \xrightarrow[\text{411 K endo}]{373-423\text{ K}} \mathrm{Sm(4\text{-}bpy)(CCl_2HCOO)_3} \xrightarrow[\text{503 K exo}]{453-548\text{ K}}$$

$$\rightarrow \mathrm{Sm(4\text{-}bpy)(CCl_2HCOO)Cl_2} \xrightarrow[\text{703, 833, 1063 K exo}]{548-1093\text{ K}} \mathrm{SmOCl} \xrightarrow[\text{1203 K exo}]{>1093\text{ K slowly}} \mathrm{Sm_2O_3}$$

MS data for the complex detected several ions. Major profiles for ion currents are observed with $m/z = 12$ (C^+), 29 (CHO^+), 30 (NO^+ or CH_2O^+), 35 (Cl^+), 36 (HCl^+), 44 (CO_2^+), 47 (CCl^+) and others. Many maxima are observed with heating at 517–610, 675–843 and 1045–1079 K. Strong CO_2^+ peaks were observed at 518, 717, 839 and 1076 K. In the range 527–822 K, several signals for fragments containing chlorine were observed. Maximum rates of formation of NO^+ (or CH_2O^+) are at 849 and 1045 K. The MS curve for $m/z = 32$ (O_2 from air) shows minima at 526, 843 and 1078 K.

Supplementary data

Tables of crystal data and structure refinement details, anisotropic displacement coefficients, atomic coordinates and equivalent isotropic displacement parameters for non-hydrogen atoms, H-atom coordinates and isotropic displacement parameters, bond lengths and angles have been deposited with the Cambridge Crystallographic Data Centre under (No. CCDC 277455).

Acknowledgements

This work was financed by funds allocated by the Ministry of Scientific Research and Information Technology to the Institute of General and Ecological Chemistry, Lodz University of Technology.

References

[1] P.J. Blower. *Annu. Rep. Prog. Chem. A*, **96**, 645 (2000).

[2] A.D. Sherry. *J. Alloy Comp.*, **249**, 153 (1997).

[3] M. Woods, Z. Kovacs, A.D. Sherry. *J. Supramol. Chem.*, **2**, 1 (2002).

[4] W.-B. Chang, B.-L. Zhang, L.-Z. Li, Y.-X. Ci. *Microchem. J.*, **55**, 287 (1997).

[5] D. Ferri, L. Forni. *Appl. Catal. B Environ.*, **16**, 119 (1998).

[6] T.N. Parac-Vogt, K. Binnemans. *Tetrahedron Lett.*, **45**, 3137 (2004).

[7] C. Gaona-Tiburcio, F. Almeraya-Calderón, J.G. Chacon-Nava, J.A. Matutes-Aquino, A. Martinez-Villafañe. *J. Alloy Comp.*, **369**, 78 (2004).

[8] H.C. Aspinall. *Chemistry of f-Block Elements*, Gordon and Breach Science Publishers, Amsterdam (2001).

[9] Y.-S. Lin, Y. Hung, J.-K. Su, R. Lee, C. Chang, M.-L. Lin, C.-Y. Mou. *J. Phys. Chem.*, **108**, 15608 (2004).

[10] K. Omata, T. Fujiwara, K. Kabuto. *Tetrahedron: Asymm.*, **13**, 1655 (2002).

[11] P. Caravan, C. Comuzzi, W. Crooks, T.J. McMurry, G.R. Choppin, S.R. Woulfe. *Inorg. Chem.*, **40**, 2170 (2001).
[12] P.S. Murphy, A.S.K. Dzik-Jurasz, M.O. Leach, I.J. Rowland. *Magn. Res. Imaging*, **20**, 127 (2002).
[13] X. Wan, P. Wedeking, M.F. Tweedle. *Magn. Res. Imaging*, **15**, 215 (1997).
[14] J.C. Frias, K.J. Williams, E.A. Fisher, Z.A. Fayad. *J. Am. Chem. Soc.*, **126**, 16316 (2004).
[15] S.R. Batten, R. Robson. *Angew. Chem., Int. Ed.*, **37**, 1461 (1998).
[16] C. Janiak. *Angew. Chem. Int. Ed.*, **36**, 1431 (1997).
[17] J. Tao, M.-L. Tong, X.-M. Chen. *J. Chem. Soc.*, *Dalton Trans.*, 3669 (2000).
[18] M.J. Zaworotko. *Chem. Commun.*, 1 (2001).
[19] C.R. Kagan, D.B. Mitzi, C.D. Dimitrakopoulos. *Science*, **286**, 945 (1999).
[20] J.S. Seo, D. Whang, H. Lee, S.I. Jun, J. Oh, Y.J. Leon, K. Kim. *Nature*, **404**, 982 (2000).
[21] F.M. Tabellion, S.R. Seidel, A.M. Arif, P.J. Stang. *Angew. Chem., Int. Ed.*, **40**, 1529 (2001).
[22] S.S.Y. Chui, S.M.F. Lo, J.P.H. Charmant, A.G. Orpen, I.D. Williams. *Science*, **283**, 1148 (1999).
[23] O.M. Yaghi, G. Li, H. Li. *Nature*, **378**, 703 (1995).
[24] M. Eddaoudi, H. Li, O.M.J. Yaghi. *Am. Chem. Soc.*, **122**, 1391 (2000).
[25] H. Li, M. Eddaoudi, T.L. Groy, O.M. Yaghi. *Am. Chem. Soc.*, **120**, 8571 (1998).
[26] H. Li, M. Eddaoudi, M. O'Keeffe, O.M. Yaghi. *Nature*, **402**, 276 (1999).
[27] T.M. Reineke, M. Eddaoudi, M. O'Keeffe, O.M. Yaghi. *Angew. Chem., Int. Ed.*, **38**, 2590 (1999).
[28] M. Kondo, T. Yoshitomi, K. Seki, H. Matsuzaka, S. Kitagawa. *Angew. Chem., Int. Ed.*, **36**, 1725 (1997).
[29] M. Kondo, T. Okubo, A. Asami, S. Noro, T. Yoshitomi, S. Kitagawa, T. Ishii, H. Matsuzaka, K. Seki. *Angew. Chem., Int. Ed.*, **38**, 140 (1999).
[30] M. Kondo, M. Shimamura, S. Noro, S. Minakoshi, A. Asami, K. Seki, S. Kitagawa. *Chem. Mater.*, **12**, 1288 (2000).
[31] S. Noro, S. Kitagawa, M. Kondo, K. Seki. *Angew. Chem., Int. Ed.*, **39**, 2082 (2000).
[32] W. Mori, F. Inoue, K. Yoshida, H. Nakayama, S. Takamizawa, M. Kishita. *Chem. Lett.*, **26**, 1219 (1997).
[33] R. Nukada, W. Mori, S. Takamizawa, M. Mikuriya, M. Handa, H. Naono. *Chem. Lett.*, **28**, 367 (1999).
[34] S. Takamizawa, W. Mori, M. Furihata, S. Takeda, K. Yamaguchi. *Inorg. Chim. Acta*, **283**, 268 (1998).
[35] K. Seki, S. Takamizawa, W. Mori. *Chem. Lett.*, **30**, 122 (2001).
[36] K. Seki, S. Takamizawa, W. Mori. *Chem. Lett.*, **30**, 332 (2001).
[37] D. Li, K. Kaneko. *Chem. Phys. Lett.*, **335**, 50 (2001).
[38] O.M. Yaghi, H. Li, T.L. Groy. *J. Am. Chem. Soc.*, **118**, 9096 (1996).
[39] O.M. Yaghi, C.E. Davis, G. Li, H. Li. *J. Am. Chem. Soc.*, **119**, 2861 (1997).
[40] H. Li, C.E. Davis, T.L. Groy, D.G. Kelley, O.M. Yaghi. *J. Am. Chem. Soc.*, **120**, 2186 (1998).
[41] T.M. Reineke, M. Eddaoudi, M. Fehr, D.G. Kelley, O.M. Yaghi. *J. Am. Chem. Soc.*, **121**, 1651 (1999).
[42] H.J. Choi, T.S. Lee, M.P. Suh. *Angew. Chem., Int. Ed.*, **38**, 1405 (1999).
[43] O.M. Yaghi, H. Li. *J. Am. Chem. Soc.*, **117**, 10401 (1995).
[44] O.M. Yaghi, H. Li. *J. Am. Chem. Soc.*, **118**, 295 (1996).
[45] O.M. Yaghi, H. Li, T.L. Groy. *Inorg. Chem.,* **36**, 4292 (1997).
[46] B.F. Hoskins, R. Robson. *J. Am. Chem. Soc.*, **112**, 1546 (1990).
[47] M. Fujita, Y.J. Kwon, S. Washizu, K. Ogura. *J. Am. Chem. Soc.*, **116**, 1151 (1994).
[48] T. Sawaki, T. Dewa, Y. Aoyama. *J. Am. Chem. Soc.*, **120**, 8539 (1998).
[49] STOE & Cie GmbH. *X-RED. Version 1.18*, Darmstadt, Germany (1999).
[50] G.M. Sheldrick. *Acta Cryst.*, **A46**, 467 (1990).
[51] G.M. Sheldrick. *SHELXL97. Program for the Solution and Refinement of Crystal Structures*, University of Göttingen, Germany (1997).
[52] G.M. Sheldrick. *SHELXTL: Release 4.1 for Siemens Crystallographic Research Systems*, Madison, WI, USA (1990).
[53] W.J. Geary. *Coord. Chem. Rev.*, **7**, 81 (1971).
[54] M.G.B. Drew. *Coord. Chem. Rev.*, **24**, 179 (1977).
[55] N.F.M. Henry and K. Longdale, eds. *International Tables for Crystallography*, Kynoch Press, Birmingham (1952).
[56] G.G. Sadikov, G.A. Kukina, M.A. Porai-Koshits. *Zh. Strukt. Khim. (Russ.)*, **8**, 551 (1967).
[57] P.C. Junk, C.J. Kepert, L. Wei-Min, B.W. Skelton, A.H. White. *Aust. J. Chem.*, **52**, 437 (1999).
[58] S. Ganapathy, V.P. Chacko, R.G. Bryant, M.C. Etter. *J. Am. Chem. Soc.*, **108**, 3159 (1986).
[59] Y. Sugita, A. Ouchi. *Bull. Chem. Soc. Jpn*, **60**, 171 (1987).
[60] H. Lei, Y. Yang, Y. Liu. *Zhongshan Daxue Xuebao Ziran Kexueban*, **59**, 2 (1990).
[61] A.G. Karipides, J. Jainhuknan, J.S. Cantrell. *Acta Cryst.*, **C52**, 2740 (1996).
[62] A. Lossin, G. Meyer. *Z. Naturforsch.*, **B48**, 886 (1993).
[63] A. Ma, L. Li, Y. Lin, S. Xi. *J. Coord. Chem.*, **33**, 59 (1994).
[64] J.-F. Ma, Z.-S. Jin, J.-Z. Ni. *Huaxue Xuebao*, **51**, 265 (1993).
[65] Y. Sugita, Y. Ohki, Y. Suzuki, A. Ouchi. *Bull. Chem. Soc. Jpn*, **60**, 3441 (1987).
[66] G. Meyer, C. Bromant. *Z. Anorg. Allg. Chem.*, **629**, 6 (2003).
[67] I.D. Brown. *Acta Cryst.*, **B48**, 553 (1992); *ibid.*, **B53**, 381 (1997).
[68] M. O'Keeffe, N.E. Brese. *J. Am. Chem. Soc.*, **113**, 3226 (1991).

[69] M. O'Keeffe, N.E. Brese. *Acta Cryst*., **B47**, 192 (1997).
[70] A. Trzesowska, R. Kruszynski, T.J. Bartczak. *Acta Cryst*., **B60**, 174 (2004).
[71] A. Trzesowska, R. Kruszynski, T.J. Bartczak. *Acta Cryst*., **B61**, 429 (2005).
[72] G.R. Desiraju, T. Steiner. *The Weak Hydrogen Bond in Structural Chemistry and Biology*, Oxford University Press, Oxford (1999).
[73] G.A. Jeffrey, W. Saenger. *Hydrogen Bonding in Biological Structures*, Springer-Verlag, Berlin (1994).
[74] R. Taylor, O. Kennard. *J. Am. Chem. Soc*., **104**, 5063 (1982).
[75] C.A. Hunter, J.K.M. Sanders. *J. Am. Chem. Soc*., **112**, 5525 (1990).
[76] C.K. Pearce, D.W. Grosse, W. Hessel. *Chem. Eng. Data*, **15**, 567 (1970).
[77] J.S. Ahuja, R. Singh, C.L. Yadava. *J. Mol. Struct*., **74**, 143 (1981).